Road Extraction From High-Resolution Satellite Images Based on Multiple Descriptors

Jiguang Dai, Tingting Zhu ⬤, Yang Wang, Rongchen Ma, and Xinxin Fang

Abstract—Geometry and texture noise make it difficult to accurately describe road image rules, which leads to the low degree of automation of traditional template matching algorithms based on internal texture homogenization. We propose a semi-automatic road extraction method based on multiple descriptors to improve the degree of automation while ensuring the accuracy of road extraction. This method aims to address the problems of incomplete road image geometric information and poor homogeneity of internal road texture. The multiscale line segment orientation histogram model and sector descriptor are established. Road points are tracked by interpolation and extension, and postprocessing is used to fit the tracking points and extract the road routes. In this article, high-resolution remote sensing images of different types, different resolutions, and different scenes are selected, and the roads exhibit curvatures, vehicle and shadow occlusions, roundabouts, and variational features. Experiments show that for roads with a certain width, completeness, and correctness of the method are more than 98%. Additionally, as compared with other algorithms, the interactive human intervention of this method is reduced by more than 2/3.

Index Terms—Line segments, multiscale analysis, multiscale line segment orientation histogram (MLSOH), road centerline extraction, sector descriptor.

I. INTRODUCTION

IN RECENT years, road extraction from remote sensing images has gradually become the main way to update road information [1]–[4]. Scholars in related fields have studied road extraction, including road area extraction [5] and road centerline extraction [6], [7]. Road area extraction is mainly based on segmentation, classification, and postprocessing. Typical segmentation methods include fuzzy C-means [8], graph-based algorithms [9], edge-based algorithms [10], threshold segmentation [11], and multiscale segmentation [12], [13]. Classification methods are based on color and shape information [14], shape and spectral features [15], pixel information [16], and contextual information [17]. Postprocessing usually uses mathematical

morphology, template matching methods [8], [18]–[20], or tensor voting [12] to optimize road extraction results. For example, Maboudi *et al.* [12] used a multiscale model combining color and shape information to segment images and structural, spectral, and texture features to classify segmentation units, and they connected road fracture zones using the tensor voting method. The classical object-oriented method has been applied in this kind of method in the eCognition software, and it has achieved a better road extraction effect in regions with little spectral texture distortion. However, since segmentation, classification, and postprocessing are usually performed in order, when local deformation leads to oversegmentation or undersegmentation, the lack of an effective feedback mechanism will inevitably lead to the misjudgment of the segmentation unit, thus reducing the accuracy of road extraction.

The road centerline extraction method focuses on the detection of the road skeleton, and two different methods are usually adopted: thinning and tracking. The thinning operation is carried out on the extracted road area [21]; interested readers can find the details of the algorithm in [15], [22], and [23]. The template matching algorithm is a typical road tracking method, and it requires to input initial information artificially and set matching rules. The local image information matches the formulated rules, and the objects are recognized. Accordingly, templates can generally be divided into regular and variable templates, among them

1) regular template: Classical templates include the profile template [24], [25], the rectangular template [26], the T-shaped template [27], and the circular template [28]. For example, Zhang *et al.* [26] manually input three points on both sides of the road, constructed a rectangular template and input direction parameters, selected the grey difference and Euclidean distance as similarity measures, determined the optimal tracking point, and extracted the road using an iterative method. This method has the advantage of high precision in road extraction, but it requires a high degree of manual participation under geometric and texture interference;

2) variable template: The commonly used models include the dynamic contour model [29], [30] and the level set model [31], [32]. For example, Nakaguro *et al.* [30] used the level set method to segment remote sensing images. The second-order moment is calculated, and the road networks are extracted using prior information about the geometric shape. This kind of method can overcome poor homogeneity in the level set method to segment remote sensing images. The second-order moment is calculated, and the road networks are extracted using prior

The authors are with the School of Geomatics, Liaoning Technical University, Fuxin 12300, China (e-mail: daijiguang@lntu.edu.cn; 1502466979@qq.com; 1613051911@qq.com; 410666523@qq.com; 312934890@qq.com).
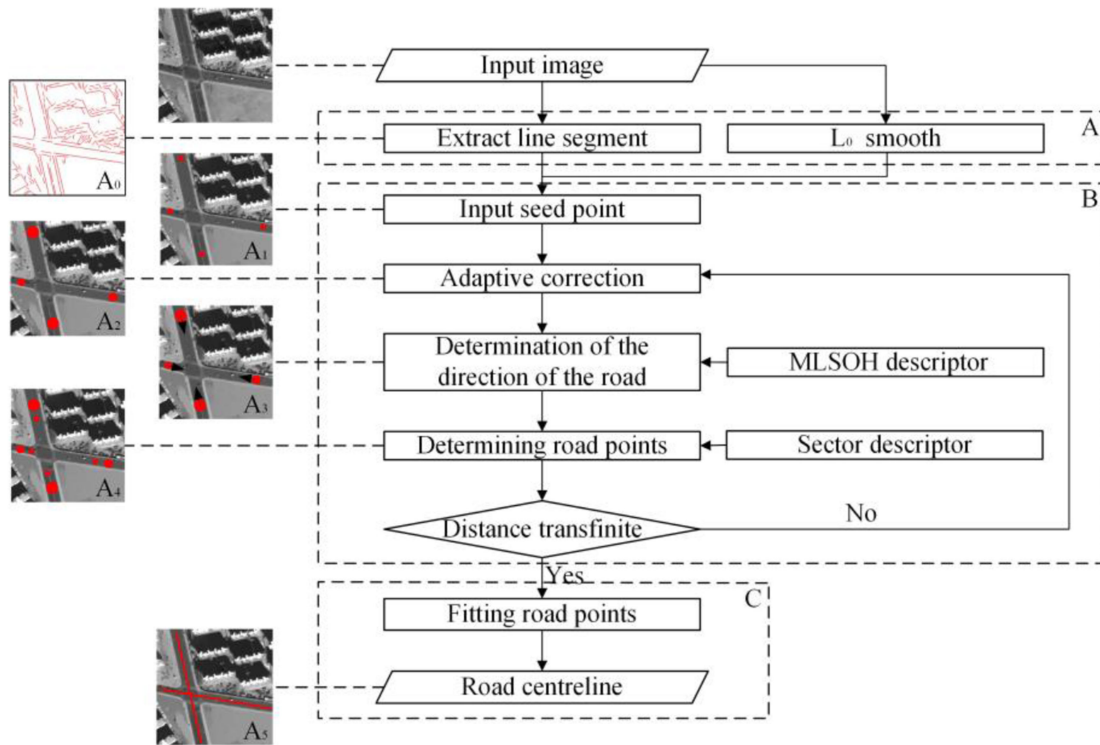
Fig. 1.   Flowchart of the proposed method, which consists of (a) preprocessing, (b) matching and tracking processes, and (c) postprocessing.

information about the geometric shape. This kind of method can overcome poor homogeneity in the road interior; however, the initial artificial input points have a great influence on the final road extraction results, and there are many problems such as a large number of artificial input points and complex calculations.

Compared with the first type of road area extraction method, the existing template matching method has high road extraction accuracy, and it has been applied in commercial software such as Erdas EasyTrace, Feature Analyst, and Easy Feature. However, as the road extraction method focuses on matching and tracking between local roads, local object occlusion, radiation difference, imaging blur, and other road image interference problems often require more interactive human intervention manual participation, which will lead to a decline in the degree of automation of road extraction. Therefore, improving the level of automation while ensuring the accuracy of road extraction is a difficult task when developing road template matching methods, and this task has been a key factor restricting the progress of template matching methods in recent years. Therefore, to solve this problem, this article proposes a high-resolution remote sensing image road extraction method combined with multiple descriptors, and it is designed as follows.

1) In the seed point input stage, to reduce the manual input of road width information, we adaptively correct the artificial input points and extract the road width information according to the texture homogeneity of the road interior.
2) In the road direction prediction stage, under incomplete road image geometric information, according to the principle that the edge direction of a motor vehicle, building, isolation zone, or traffic indication line in a road buffer zone

is close to the road direction, a multiscale line segment orientation histogram descriptor (MLSOH) is proposed to determine the road tracking direction.
3) In the confirmation of road tracking points stage, to address the poor homogeneity of the road image internal texture caused by ground object interference, according to the idea that the texture difference between the road surface area and the road/nonroad mixed area is large, a sector descriptor is constructed to verify the road direction and determine the best road tracking point.
4) In the postprocessing stage, to handle low-precision track points, the least squares method is used to optimize the road points and extract the road centerline.

II. METHODS

A flowchart of the proposed method is depicted in Fig. 1, which shows three main stages of the proposed method: (a) preprocessing, (b) matching and tracking processes, and (c) postprocessing. Preprocessing consists of two major steps: 1) line segment extraction (see Fig. $1A_0$) and 2) L_0 smooth filtering. The steps in the process of road-point tracking are as follows. First, the starting point and end point of the road are input (see Fig. $1A_1$), and the adaptive road parameter acquisition model is used to obtain the coordinates of the road center point and the radius of the road (see Fig. $1A_2$). Second, the road direction is determined according to MLSOH descriptor (see Fig. $1A_3$), and the sector descriptor is used to verify the road direction and determine the best road points (see Fig. $1A_4$). Finally, the matching and tracking of road points is completed
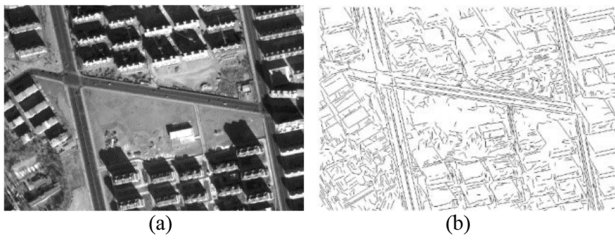
Fig. 2. Line extraction result. (a) Input image. (b) Result of line extraction.

by iterative interpolation. In the postprocessing step, the least squares principle is used to optimize the road points and obtain the centerline of the road (see Fig. 1A$_5$).

A. Preprocessing

In this article, preprocessing consists of two steps: extracting line segments based on the original image to ensure the accuracy of the information [the results are shown in Fig. 1(A$_0$)] and filtering the image with L_0 smoothing to improve the homogeneity of the pixels inside the road and enhance the difference between road and nonroad features. However, although the filtering process can filter out noise and improve the pixel homogeneity of the road, the structural information of the road is weakened. Therefore, the two preprocessing steps in this article are independent of each other.

1) Line Segment Extraction: Filtering usually leads to edge blurring. Therefore, based on the original image, this article directly uses the method proposed by Dai *et al.* to extract straight line segments [38]. The linear segment is selected mainly because of its strong direction and length information, which can help to interpret the structural information of the road area. First, for this method, a complete refinement algorithm targeting the Canny edge map was presented. Second, an improved chain code tracking method was proposed, and the key algorithm steps are as follows: the start points of the chain code are detected; the main dynamic directions are set up to determine the tracking direction of the chain code; the edge points inside the eight neighborhoods are tracked (or the edge points outside the eight neighborhoods are tracked if there are no edge points inside the eight neighborhoods); linear analysis is employed to perform dynamic constraints on the chain code; and linear fitting and phase marshaling validation are applied after chain code tracking (straight lines are output when conditions are satisfied; otherwise, the start point of the chain code should be reset to extract straight lines).

As shown in Fig. 2(b), at the edge of the road, the line segment extracted from the centerline of the road and parts of the shadows of some buildings have the same or similar directions, which makes it possible to track the road based on the line segments. In the following section, the MLSOH descriptor is created based on seed point information and line segment information (direction, length, and topological information).

2) L_0 Smoothing: In high-resolution remote sensing images, a main road has uneven surface brightness. For example, with a ground sampling distance (GSD) of less than 1 m (the GSD
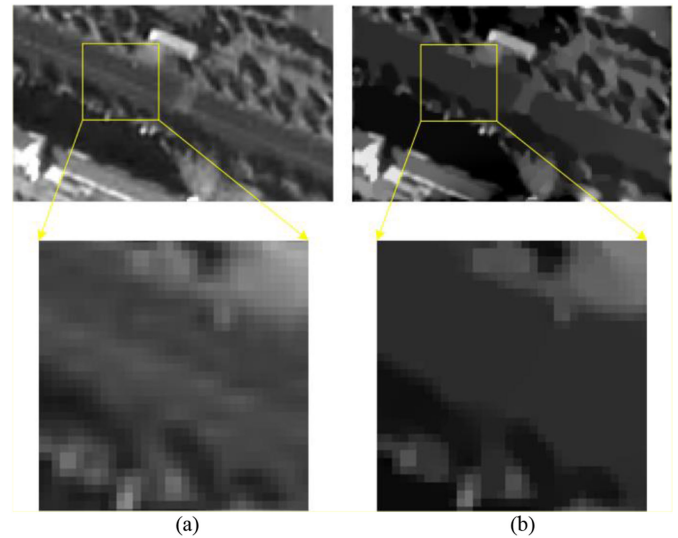

Fig. 3. L_0 smoothing result. (a) Input image. (b) Result of filtering.

of Fig. 3 is 0.8 m), zebra crossings, vehicles, and many other small details are visible [see Fig. 3(a)]. These factors increase the complexity of pavement texture analysis. In this article, L_0 smooth filtering [34] is used to eliminate unimportant details by removing small nonzero gradients, which enhance the saliency of the image to preserve the road boundary information.

As shown in Fig. 3(b), the noise and zebra crossing were removed, and the pavement texture exhibited homogeneity. The contrast between the road surface and the surrounding environment was also enhanced, and the road edge information was well preserved.

B. Matching and Tracking Process

We propose a multidescription road extraction model. First, the road width and center point information are obtained by an adaptive road parameter acquisition model (see Fig. 1A$_2$). Second, MLSOH descriptors are established to predict the direction of road tracking (see Fig. 1A$_3$). Third, the road tracking points are extracted by sector descriptors (see Fig. 1A$_4$). Finally, road tracking is completed through interpolation and extension.

1) Adaptive Road Parameter Acquisition Model: Seed points are the basic initial information extracted from roads. As shown in Fig. 1A$_1$, using manual input seed points, we can obtain the position and width information of road center points, and these seed points also serve as a reference for template matching. Therefore, selecting seed points on a road section with clear edges but without vehicle and shadow effects is necessary. To automatically obtain accurate road width and texture information, while inputting seed points, the artificial input points cannot be accurately located in the center of the road due to the limitation of subjective factors. Thus, in this article, the gradient constraint is used to modify the seed points [35] to obtain the position of the road center and the road width. The specific steps are as follows.

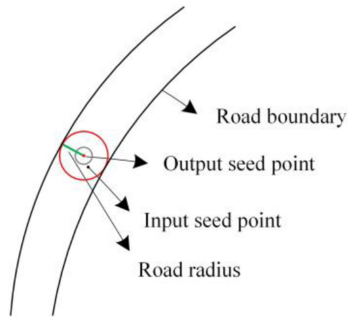1) Create a circular template with a radius of one pixel centered on the input point.

Fig. 4.   Seed point fitting diagram.

2) Automatically search for the eight neighborhood pixels of the input points and take each pixel as the center to create a circular template with the same size as that in 1).

3) Compare the sums of the morphological gradients in each template and take the smallest gradient value as the most suitable template for this radius.

4) Estimate whether the sum of the gradients in the most suitable template exceeds the gradient threshold (μ); if not, then the radius (in pixels) of the circular template is increased, and , 2) and 3) are repeated until the gradient threshold is exceeded. The final template is the size of the standard template, the center point of the template is taken as the road center point, and the diameter of the circular template is taken as the width of the road.

Fig. 4 shows the adaptive extraction process of road parameters; the result is shown in Fig. 1(A_2). The red point is the final standard template, the green line is the radius of the road, and the red point is the corrected center point of the road.

2) Establishment of the MLSOH Descriptor:

a) Analysis of the descriptor parameter: In actual scenes, local roads have typical directionality, which can be reflected only from the direction of the edge lines on both sides of the road in low-resolution remote sensing images. However, in high-resolution remote sensing images, this directivity can be reflected from the edges of relevant ground objects in multiple regions. First, inside the road, the road markings, edges of moving motor vehicles, isolation zones, and edges of the shadows of flat-top buildings have a direction that is the same or similar to road; second, at the edge of the road, the rule tree, edges of parked vehicles, and edges of adjacent buildings all have the same direction as the road; finally, near the road, the edges of buildings usually have directions similar to that of the road. In the process of template matching design, this article attempts to introduce this rule into the process of determining the road tracking direction, and it interprets the road direction by taking advantage of the idea that the edge direction of a variety of ground objects is the same as the road direction.

Edge information includes edge points and edge lines [36]. Edge points are discrete information, their regularity is difficult to express, and noise interference is relatively severe. Edge lines are sets of edge points that conform to a certain regularity that has directionality, and they are less disturbed by noise. As shown in Fig. 5, this article establishes a rectangular search area with two times the width of the road as the side length, and the
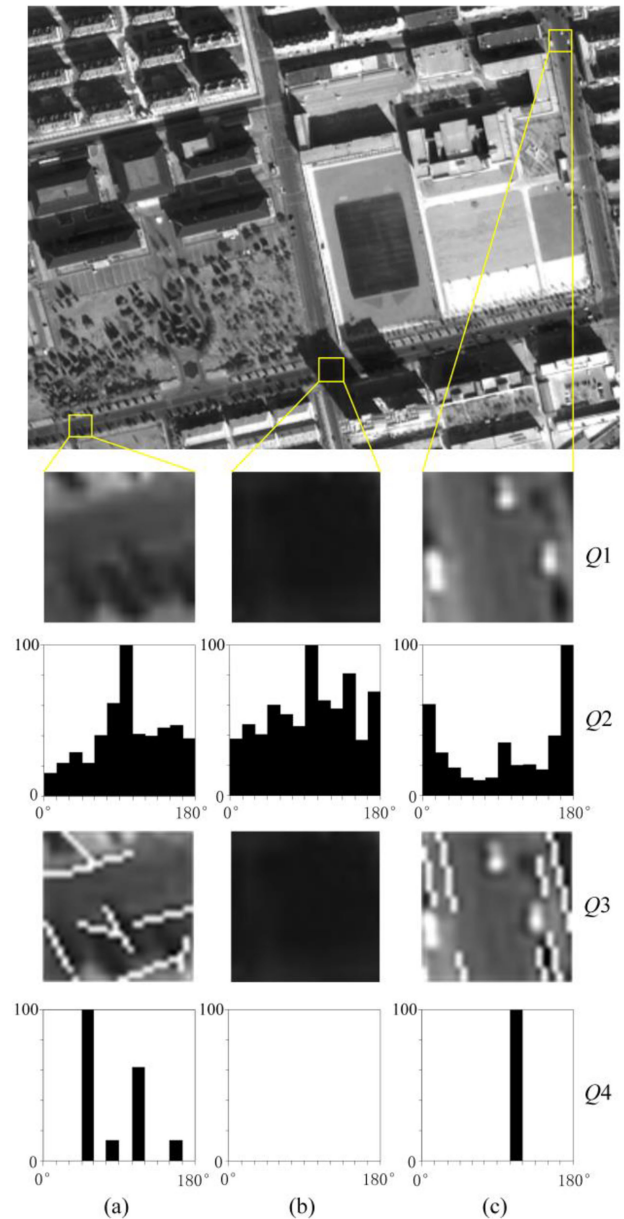

Fig. 5.   Rectangular search area diagram. (a) Half-sheltered road. (b) Fully sheltered road. (c) Road with many vehicles. Q1: Enlarged view of the corresponding region. Q2: Histogram of the gradient directions. Q3: Results of line segment extraction. Q4: Histogram of the line segment directions.

semi-occlusion section [see Fig. 5(a)], the full occlusion section [see Fig. 5(b)] and the multivehicle section [see Fig. 5(c)] are selected to conduct statistics on image edge points and edge lines. Images Q1–Q4 show enlargements of the corresponding regions, histograms of the gradient directions, the results of line segment extraction, and histograms of line segment directions (Statistical angles range from $0°$ to $180°$, and this range is divided into 12 equal parts of $15°$; each $15°$ is treated as an angle band). It can be seen from Q2 in Fig. 5 that the gradient direction of the pixel cannot represent the direction of the road due to the influence of noise, and the peak value is significantly different from the road direction. In contrast, in Q4 in Fig. 5, in the semi-occluded road and the multivehicle section, the peak of the
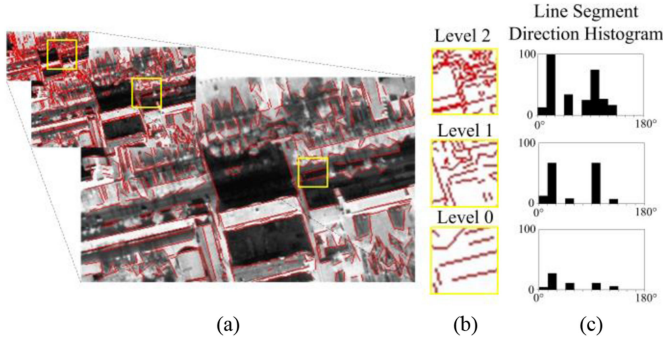
Fig. 6. MLSOH descriptor. (a) Line segment pyramid building diagram. (b) Enlarged view of the rectangular search area of each pyramid. (c) Line segment orientation histogram

Fig. 7. Sector descriptor.

histogram in the line direction is consistent with the direction of the road.

b) Principle of the MLSOH descriptor: In this article, the multiscale pyramid method is used to determine the direction of the road. By using this method, when the size of the rectangular search area remains unchanged, with the change in spatial scale, the accuracy of line segment's ability to express structural information can be improved, and the problem of increasing complexity caused by the expansion of search scope can be overcome. The MLSOH descriptor is established as follows.

1) A line segment pyramid is constructed. The coordinates of the end point of line segments (0 level), which detected by the original image, are mapped to level 1 and level 2 such that reductions of 1/2 and 1/4, respectively.

2) On level 0, a rectangular search area is established with two times the width of the road as the side length; the center points of the search area are reduced by 1/2 and 1/4, respectively, and large rectangular search areas of the same size as level 0 are established at the corresponding positions on levels 1 and 2.

3) The total lengths of the line segments in each direction in each search area are counted separately, and the direction histogram of the line segment is established. The transverse axes are grouped by the direction of the line segments; the scale unit is 15°, and the angle range is 0°–180°. The vertical axis is the cumulative value of the length of the line segment, and the unit is the pixel.

4) The road direction is determined according to the peak information of the line segment histogram.

In this article, the pyramid has three levels because the experimental analysis shows that the top level of the three-level pyramid is eight times the actual width of the road, which is enough to represent the road neighborhood. If the number of levels is expanded, the other edges of the non-road area will be easily highlighted, which is not conducive to the prediction of the direction of the road. As shown in Fig. 6, the tracking direction is from right to left. In the location of the search area in the figure, some roads are blocked by the shadow of the building and there is considerable noise on the road boundary; thus, road boundaries provide little line information. However, the shadow
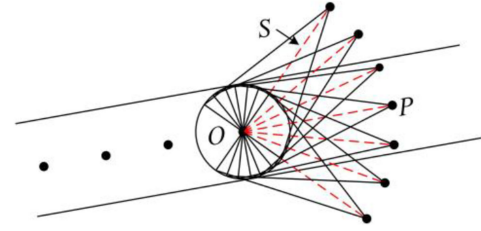
boundary, which is usually regarded as noise, is consistent with the direction of the road boundary. The MLSOH descriptor complements the road boundary information by capturing such information so that the correct road direction can be obtained at level 0. Comparing the histograms of the line segments of level 1 and 2, we can see that the road direction is still at the peak, which fully indicates the stability of the line direction histogram. Thus, formula (1) will be satisfied, and the corresponding direction can be determined

$$\text{Heap\_}f \geq \lambda \times \text{Heap\_}s. \qquad (1)$$

In formula, Heap_*f* is the maximum value in the line segment histogram in pixels. Heap_*s* is the subpeak in the line segment histogram in pixels; λ is a proportional factor.

The introduction of the multiscale based on the MLSOH descriptor can ensure the stability of the road direction in regions with complex linear features and small shadow occlusions.

3) Sector Descriptor: Although the MLSOH descriptor can determine the direction of a road, the road direction determined by the descriptor is calculated based on 15° increments. Thus, the direction may have a slight deviation, and when the road conditions are complicated (detours, intersections, and roundabouts), the accuracy of direction prediction is insufficient. Therefore, according to the homogeneity of the road interior texture and the difference between road and nonroad features, a sector descriptor is constructed by combining seven triangles (see Fig. 7). The steps for constructing a sector descriptor are listed as follows.

1) With the current tracking point as the center, the road width as the bottom, the point *P* as the vertex, and the *OP* as the centerline, an isosceles triangle is established along the road direction. The distance *S* between *O* and *P* is 3 times the road radius.

2) The triangle is rotated around the center *O* by ±15°, ±30°, and ±45° to obtain six triangles.

3) In this article, the mean gray level ($\text{Gray}_{\text{average}(i)}$), the sum of the gradients ($\text{Grad}_{\text{sum}(i)}$), and the position angle (θ_i) in each triangle are used as statistical units. The range of *i* is 0–6 for each triangle from top to bottom, respectively. θ_i is the angle between the vertex of each triangle and *O*.

The reason why *s* is set to three times the road radius and the rotation angle is set to 15° is to ensure that at least two triangles are on the road when the road radius is greater than or equal to 3 pixels, increasing the stability of the algorithm.
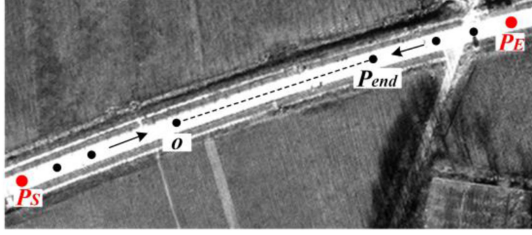
Fig. 8. Tracking process diagram.

4) Tracking Mode: Taking the seed point as a starting point, the road seed point is tracked by an iterative method, which is a common way for the template matching to extract road seed points. Commonly used tracking methods include iterative interpolation methods [37] and bidirectional iteration methods [38]. The bidirectional iterative tracking method needs to determine only the two adjacent points, which is convenient and fast. However, it is difficult to effectively control the tracking direction during tracking, and thus, road extraction errors can easily occur. Therefore, the iterative interpolation method is selected for matching tracking, and the regions from the starting point and the ending point of the road to the middle of the road are traced simultaneously. As shown in Fig. 8, P_S is the starting point, P_E is the ending point, O is the current tracking point in the starting direction, and P_{end} is the current tracking point in the ending direction. In the tracking process, the matching process of different descriptors is as follows.

1) The MLSOH descriptor is used to determine the direction of the road. In general, MLSOH can directly determine the road direction by using the peak value. When complex road image features such as blurred images, trees, buildings, and shadows lead to line breakage or make the line direction deviate from or be perpendicular to the road direction, double-peak, multipeak, and no-value phenomena can occur, as shown in the histogram of the direction of the line segment constructed according to the level 0 pyramid. For double-peak and multipeak phenomena, if the main peak of the histogram satisfies the formula (3), it is the road direction. Otherwise, the subpeak is judged. When the peak of the line segment in the 0- level histogram is not prominent, we analyze level 1 and level 2 in turn

$$\theta = \text{average}\left(\theta_{S_{i-5}} : \theta_{S_i}\right) \tag{2}$$

$$abs(\varphi - \theta) \leq \alpha. \tag{3}$$

In formula (2), $\theta s_{i-5} : \theta s_i$ represents the angle of the nearest six tracking points (θs_i is the angle between P_{Si} and point P_{Si-1}) in the starting point direction, and θ is the average angle of the six tracking points. In formula (3), φ is the histogram peak value, and α is the angle threshold. For this formula, the angle of a tracking point with a longer distance has less reference significance to the current position, while the adjacent seed point has more guiding significance to the current tracking direction.

2) The sector descriptor is used to verify the road direction and determine the best road point. First, the difference between $\theta_{\text{reference}}$ and θ_i is calculated, and the two triangles with the largest difference are deleted. $\theta_{\text{reference}}$ is the angle between the origin O and P_{end} (see Fig. 8). The three triangles with the largest Grad_{sum} and the largest difference from the $\text{Gray}_{\text{average}}$ of the known points are removed; thus, two stable triangles can be obtained. Generally, a point on the road is significantly different from at least one side of the road in terms of grey level, and the point satisfying this condition is the best road point. If both points satisfy this condition, the point with the smaller difference between $\theta_{\text{reference}}$ and θ_i is the best road point. The optimal road point is calibrated to the center of the road by the adaptive road parameter acquisition model, and the tracking point is obtained.

3) Steps 1 and 2 are repeated until the distance between the nearest tracking points in the starting and ending directions is less than the distance threshold D is; then, tracking ends.

4) The road points are extended. Due to the selection of seed points and the requirements of MLSOH descriptor creation, the seed points in the image are not at the end of the road. Therefore, it is necessary to use the same road point tracking method to trace the road points back to the start and end points until the image boundary or road end point is reached.

C. Postprocessing

Due to the complexity of the road and the noise during image processing, error extraction is inevitable during road extraction. Thus, as shown in Fig. 1A$_5$, postprocessing is used to eliminate the effects of misinterpreted points.

At present, there are many curve fitting algorithms, among which the cubic spline curve algorithm and the least squares fitting method are commonly used. The spline curve algorithm is an interpolation algorithm that requires the curve to pass through all control points. The least squares method searches for the function corresponding to the minimum of the sum of squared errors and does not require the curve to pass through all control points. Since the purpose of postprocessing is to reduce or eliminate the influence of incorrect points on the total experimental results using correctly extracted road points, the road presents a relatively stable effect (as a whole, not just locally) and does not strictly require the curve to pass through all control points. Therefore, this article adopts the least squares (polynomial) fitting method to process the experimental results.

In the least squares method, according to the m given points, the approximate curve $y = f(x)$ of the curve $y = \varphi(x)$ is employed. The specific algorithm is expressed as follows:

$$y = a_0 + a_1 x + \cdots + a_k x^k. \tag{4}$$

The sum of the distance from each point to this curve, that is, the sum of the squared deviations (R^2), is expressed as follows:

$$R^2 = \sum_{i=1}^{n} \left[y_i - \left(a_0 + a_1 x_1 + \cdots + a_k x_i^k\right)\right]^2. \tag{5}$$

In (5), k refers to the highest order of polynomial. To obtain the a value that satisfies the condition, the partial derivative of a_i on the right-hand side of the equation is determined and represented
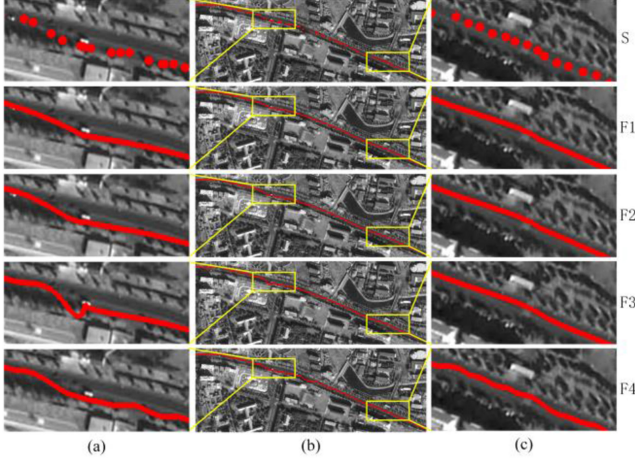
Fig. 9. Fitting parameter selection. (a) First interface enlargement of two sets of seed points. (b) Overall result. (c) Second interface enlargement of two sets of seed points. S: Results of road point selection. F1: Fitting results for road points at $k = 7$. F2: Fitting results for road points at $k = 9$. F3: Fitting results for road points at $k = 11$. F4: Fitting results for road points by a cubic spline curve.

in the form of matrix a. The following matrix can be obtained:

$$
\begin{bmatrix}
n & \sum_{i=1}^{n} x_i & \cdots & \sum_{i=1}^{n} x_i^{k} \\
\sum_{i=1}^{n} x_i & \sum_{i=1}^{n} x_i^{2} & \cdots & \sum_{i=1}^{n} x_i^{k+1} \\
\vdots & \vdots & \ddots & \vdots \\
\sum_{i=1}^{n} x_i^{k} & \sum_{i=1}^{n} x_i^{k+1} & \cdots & \sum_{i=1}^{n} x_i^{2k}
\end{bmatrix}
$$
$$
\times
\begin{bmatrix}
a_0 \\
a_1 \\
\vdots \\
a_n
\end{bmatrix}
=
\begin{bmatrix}
\sum_{i=1}^{n} y_i \\
\sum_{i=1}^{n} x_i y_i \\
\vdots \\
\sum_{i=1}^{n} x_i^{k} y_i
\end{bmatrix}. \tag{6}
$$

With the reduction of this matrix, the following matrix can be obtained:

$$
\begin{bmatrix}
1 & x_1 & \cdots & x_1^{k} \\
1 & x_2 & \cdots & x_2^{k} \\
\vdots & \vdots & \ddots & \cdots \\
1 & x_n & \cdots & x_n^{k}
\end{bmatrix}
\begin{bmatrix}
a_0 \\
a_1 \\
\vdots \\
a_k
\end{bmatrix}
=
\begin{bmatrix}
y_1 \\
y_2 \\
\vdots \\
y_n
\end{bmatrix}. \tag{7}
$$

That is, $X * A = Y$; then, $A = (X' * X)^{-1} * X' * Y$, and we obtain the coefficient matrix A and the fitting curve.

Considering detours and roundabouts, we grouped the road points of a road; a group consisted of 40 points (if the last group of road points was less than or equal to 20, then these points were classified into the previous group; otherwise, the points were separately grouped).

F4 in Fig. 9 shows that the results of the spline curve are closest to the control point and have strong stability, but this algorithm does not play a role in reducing the error at the control point; in

addition, the local smoothing effect of this algorithm is the best, but in a larger range, the results still show a bending state; thus, this algorithm cannot achieve the purpose of the postprocessing steps in this article. According to the formula of polynomial fitting, in theory, the greater the number of polynomial terms, the more accurate the result. However, for high accuracy, the number of calculations is large. Additionally, (F3) in Fig. 9(a) shows that when $k = 11$, the "Runge phenomenon" occurs. When $k = 7$ or $k = 9$, the fitting effect connections among road points of different groups are good, and the results are in line with the seed point when the order of the polynomial $k = 9$.

III. EXPERIMENTAL RESULTS AND ANALYSIS

To verify the effectiveness of the method, an extensive experiment was conducted on urban and rural road extraction using four sets of data, including two GF2 satellite images and two Pleiades satellite images. Spectral information was not used in the experiments, and all images were panchromatic images. All data underwent radiation correction without georeferencing and geometrical correction.

A. Experimental Setup

1) Parameter Settings: The template matching method is a solution to the local road self-similar problem, that is, the best match between the existing road area and the predicted road area is obtained. Therefore, although the geometric and texture features of different roads or different sections of the same road will change greatly, there is great similarity among the geometric textures of local roads. Therefore, locally, experimental parameters are set according to the robustness, and globally, these parameters have fixed values.

The proposed algorithm needs four parameters, including gradient threshold μ in the road parameter adaptive extraction model, proportional factor λ in the MLSOH descriptor, angle threshold α and distance threshold D is in the tracking process.

1) For μ, the texture inside the filtered image pavement has high homogeneity, and the mutation of the gradient is the road boundary. After many experiments, when the μ value is in the range from 100 to 1000, and the results are not significantly different; considering fault tolerance and accuracy, the μ value is set to 400 in this article.
2) For the peak statistical proportional factor λ, because the MLSOH descriptor mainly shows the relationship between the peak value of the line segment and the direction of the road in the region, to highlight the directivity of the edge, the threshold λ is set to 1.5 through many experiments.
3) For the angle threshold α, there is a linear feature in the local area of the road, and the angle changes slightly. Even in a large curved area, the corner of the road within two times the road radius will not exceed 30°; thus, α is set to 30 in this article.
4) For the distance threshold D is, since the widths of different roads are inconsistent; it is set to four times the road radius in this article.

2) Evaluation Metrics: Wiedemann *et al.*'s [39], [40] quality evaluation method is selected to evaluate the experimental results. The completeness ratio, correctness ratio, and root mean square (RMS) are selected to evaluate the road extraction results. The formulas for these three indicators are presented as follows.

Completeness is the ratio of the total length of the extracted road to the total length of the actual road in an image

$$\text{Completeness} = \frac{D}{D + N}. \tag{8}$$

Correctness is the ratio of the correct extracted road length to the extracted total length

$$\text{Correctness} = \frac{D}{D + E}. \tag{9}$$

The RMS, which measures the geometric quality of the detected centerlines, is defined by the following equation:

$$\text{RMS} = \sqrt{\frac{\sum_{i=1}^{n} d^2}{n}}. \tag{10}$$

In the equations, D represents the actual length of the road in the image, N is the length of the reference centerline that was not detected by the algorithm and E is the length of the segments that were classified as the centerline but are errors.

Based on quality evaluation, to demonstrate the automation advantages of our proposed method, we select the interactive human intervention degree, i.e., the number of manual input points, as the evaluation index, and the smaller the quantity, the better the automation degree.

3) Compared Methods: To verify the performance, the proposed method is compared with three related methods: the IMAGINE EasyTrace module in ERDAS9.2 (a remote sensing image processing system developed by Intergraph Company, USA), the object-oriented module in eCognition (intelligent image analysis software developed by Definiens Imaging Company, Germany) and the T-shaped template matching method proposed by Lin [27]. The EasyTrace module requires seed points to be manually input and define and specific features or targets to be specified by tracking the elements between some points. Then, the digitization of ground objects between other points can be completed automatically through the matching degree between ground objects and features or targets, which is a relatively mature template matching algorithm. The object-oriented module in eCognition is a typical object-oriented method that considers a series of factors such as spectral statistical features, shape, size, texture, and aspect ratio and completes road extraction through a segmentation and classification sequence. The T-shaped template combines the advantages of profile matching and template matching, uses the angular texture feature to accurately locate the initial road point, accurately measures the road width and the forward direction of the road, and uses least squares matching to obtain the optimal road point. It is a typical semi-automatic road extraction algorithm.

B. Results

1) GF2 Satellite Image Data: Experiment one: The data cover large urban areas, and the images are $2000 * 2000$ pixels in size with a spatial resolution of 0.8 m per pixel. The road images are complex, the difference between the road surface and the background is not prominent, the surfaces of many roads are blocked by the shadows of buildings and trees, and the shadows on some road sections cover the entire road surface.

Fig. 10(b)–(d) show the effects of different descriptors on the results. As shown in Fig. 10(b), a single MLSOH descriptor can obtain good experimental results in areas with strong road structure information. However, in the weak edge area disturbed by trees and vehicles, the linear information is not prominent enough, which leads to the tracking point deviating from the road when the rectangular descriptor is used alone. Once the tracking point deviates from the road, the subsequent determination of the road direction by the MLSOH descriptor may always be in the wrong direction. Therefore, 52 seed points need to be input manually when using only the MLSOH descriptor to ensure the effectiveness of road tracking. Fig. 10(c) shows the results based on the MLSOH descriptor and the sector descriptor. Since the sector descriptor adjusts the direction determined by the MLSOH descriptor, the accuracy is greatly improved; thus, only 14 seed points need to be input to obtain a road network. However, some road points are not in the strict road center; for example, in Fig. 10(c), there are 7 error point concentration areas with a total of 45 error points. Finally, the least squares polynomial is used to fit the road points. Fig. 10(d) shows the results of the fitting, the road lines of the two error areas are corrected, and the accuracy of road lines in other areas is also improved, which shows the coherence of different descriptors in this article.

Through the above analysis, the consistency of the different descriptors selected in this article is shown. At the same time, it can be seen from the scene analysis that, as shown in Fig. 10(d), the method in this article has a good noise resistance to shadows and can extract most of the shaded road centerlines. The first enlarged view of Fig. 10(d) shows that the road is affected by the trees on both sides, which makes the internal texture homogeneity of the road decrease, and the edges are blurred. The MLSOH descriptor alone presents a road-point extraction problem; therefore, it is necessary to supplement the seed points in this section. The MLSOH descriptor can be effectively adjusted based on the original peak value through the verification of the sector descriptor so that the road segment can be automatically tracked. The second enlarged view shows that there is an isolation line in the middle of the road, which decreases the texture homogeneity of the road surface; however, the edge of the isolation line has a good directional effect on the road. Therefore, both Fig. 10(b) and (c) can better cross the road section, which also shows that the method proposed in this article is robust when the road width changes abruptly. The third enlarged view shows that the road is blocked by the architectural shadow. This article uses the MLSOH descriptor to capture the approximate direction provided by the shadow boundary and uses the sector descriptor to analyze the difference information inside and outside the road to achieve the span of the shadow region. Therefore, by comparing the three local scenes, the proposed method has good robustness and reduces the participation of human beings when the road is disturbed by trees, blocked by shadows, or
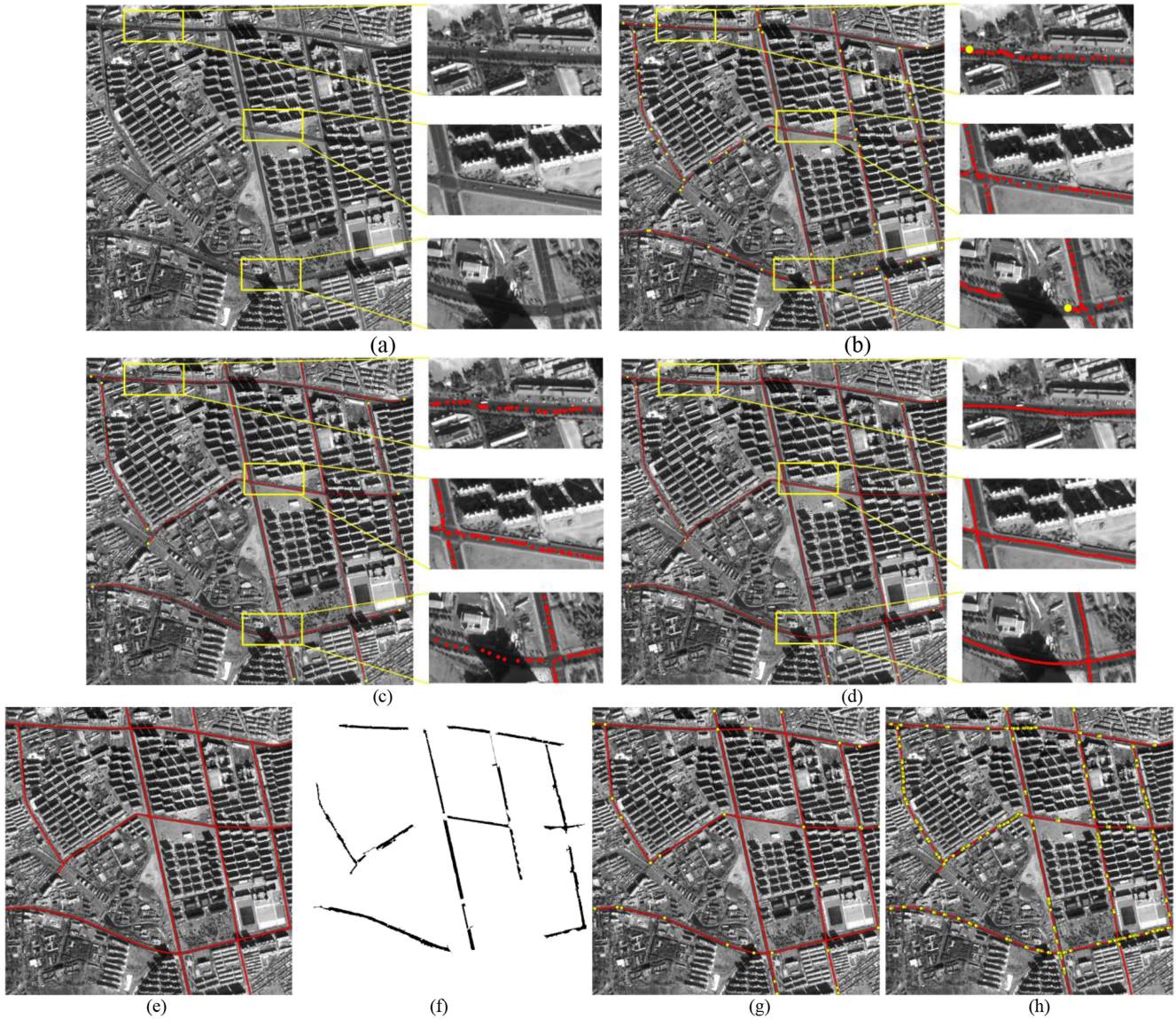
Fig. 10. First study area. (a) Input image. (b) Results using the MLSOH descriptor alone. (c) Results using the MLSOH descriptor and sector descriptors. (d) Results using least squares polynomial fitting to the road points. (e) Overlaid ground truth data. (f) Results from eCognition. (g) Results from ERDAS. (h) Results of the T-shaped template matching method.

TABLE I
EVALUATION TABLE OF THE ROAD EXTRACTION EFFECT OF EXPERIMENT ONE

Method	Proposed method	ERDAS method	eCognition method	T-shaped method
Completeness (%)	98.73	97.5	61.28	97.82
Correctness (%)	99.54	98.34	98.60	98.05
RMS (pixels)	2.20	2.78	3.31	3.63
Time (s)	68.32	218.48	80.79	238.39
Number of seeds point	14	32	0	510

TABLE II
EVALUATION TABLE OF THE ROAD EXTRACTION EFFECT OF EXPERIMENT TWO

Method	Proposed method	ERDAS method	eCognition method	T-shaped method
Completeness (%)	98.34	96.61	87.29	96.78
Correctness (%)	99.65	98.39	71.67	96.93
RMS (pixels)	1.34	2.45	4.87	2.68
Time (s)	72	227	84	167
Number of seeds point	14	60	0	288

changes in width. As shown in Table I, compared with other methods, the object-oriented method has a low road recall rate, and the shadow area road cannot be detected. Meanwhile, for the T-shaped template and the EasyTrace module, two template matching methods that require human interaction, there is too much human involvement, which can be clearly reflected by the amount of input from the seed point. While the method in this article guarantees that the accuracy of road extraction is higher than those of T-shaped template and the EasyTrace module, the number of manual input points is only 14, which is
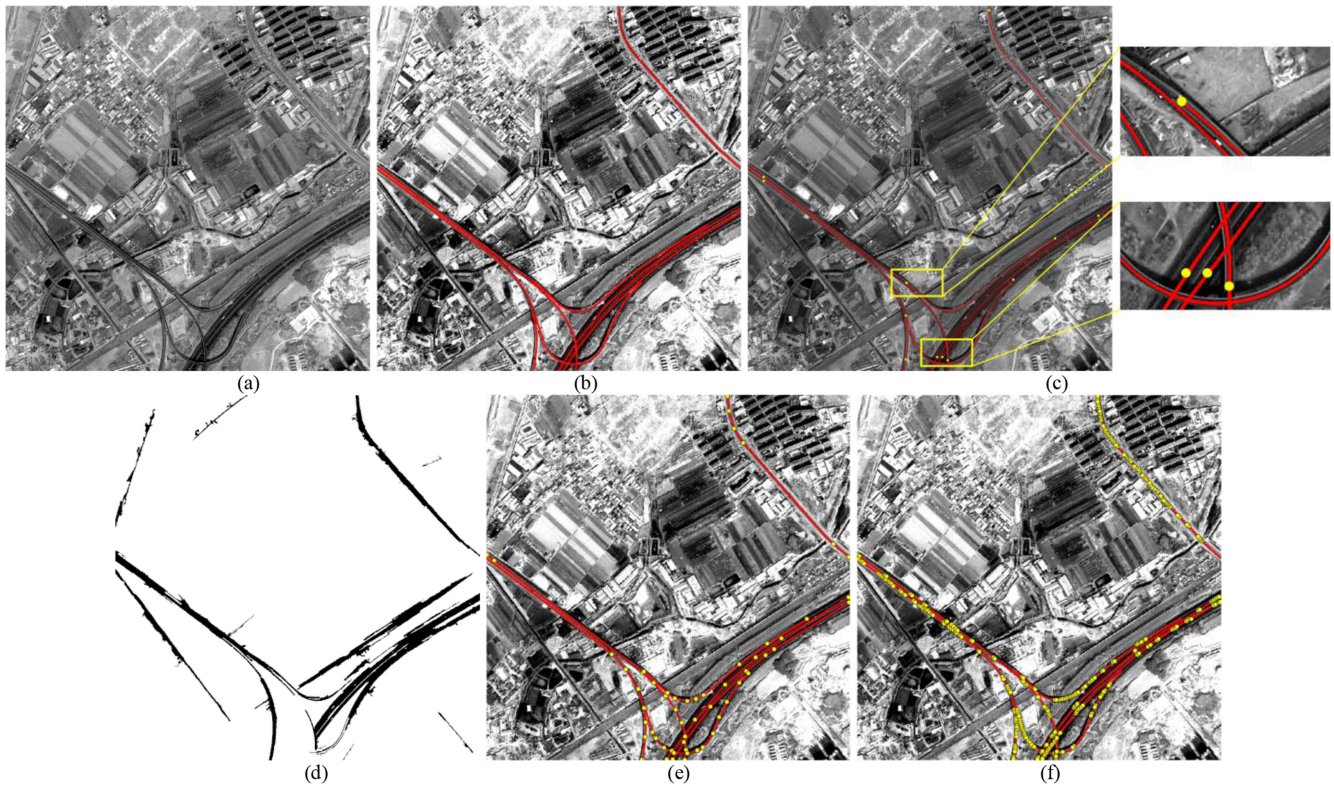
Fig. 11.   Second study area. (a) Input image. (b) Overlaid ground truth data. (c) Results of the proposed method. (d) Results from eCognition. (e) Results from ERDAS. (f) Results of the T-shaped template matching method.

TABLE III
EVALUATION TABLE OF THE ROAD EXTRACTION EFFECT OF
EXPERIMENT THREE

Method	Proposed method	ERDAS method	eCognition method	T-shaped method
Completeness (%)	98.94	96.41	88.44	97.87
Correctness (%)	99.61	97.96	87.74	98.61
RMS (pixels)	0.85	1.2	2.26	1.76
Time (s)	35	105	43	29
Number of seeds point	14	64	0	64

significantly lower than the 510 and 32 of the T-shaped template and the EasyTrace module, and the processing time is greatly compressed, indicating that our method improves the degree of automation of the algorithm.

Experiment two: The residential area shown in Fig. 11(a) is part of the urban area in Huludao. The size of the image is 2000×2000 pixels with a spatial resolution of 0.8 m per pixel. The first enlarged view, as shown in Fig. 11(c), is a variational road with two forward directions, the road changes from a two-lane road to a one-lane road, and the width of the road decreases. In this article, we first track the left road with a small change in the overall direction, determine the road direction through the MLSOH descriptor, and ensure road tracking in the predetermined direction through the angle constraint in the sector descriptor. In the second enlarged view of Fig. 11(c) with a larger curvature, the method of the present invention can

automatically extract the road segment. Similarly, as shown in Fig. 11(e) (ERDAS software method) and (f) (T-shaped template), it can be clearly seen that the road segment requires a large number of supplementary points, and the degree of automation is very low. It can be shown that this method can maximize the degree of automation of the algorithm while guaranteeing the accuracy of road extraction.

2) Pleiades Satellite Image Data: Experiment three: The data cover country areas, and the images are 2000×2000 pixels in size with a spatial resolution of 0.5 m. In the image, the main route consists of one main road and two branches. The first enlarged view in Fig. 12(c) is a section with a large curvature, and the curve is shaded. The road structure features are not obvious here. Using the sector descriptor to analyze the difference between the inside and outside of the road, the tracking point can be obtained, and the shadow can be crossed, which can indicate the necessity of the sector descriptor. The second and third enlarged views are straight roads and curved roads under the occlusion of irregular trees. The texture similarity between this road sections and the adjacent surface features is great, and the difference between inside and outside the road is not obvious. Therefore, the object-oriented algorithm in Fig. 12(d) has a poor extraction effect on these segments, and it is difficult to ensure the accuracy of road extraction. In this article, the MLSOH descriptor is used to capture a small amount of clear road boundaries and structural information provided by buildings near the road and determine the direction of the road. The sector descriptor is used to select the most suitable road points and extract such road segments.
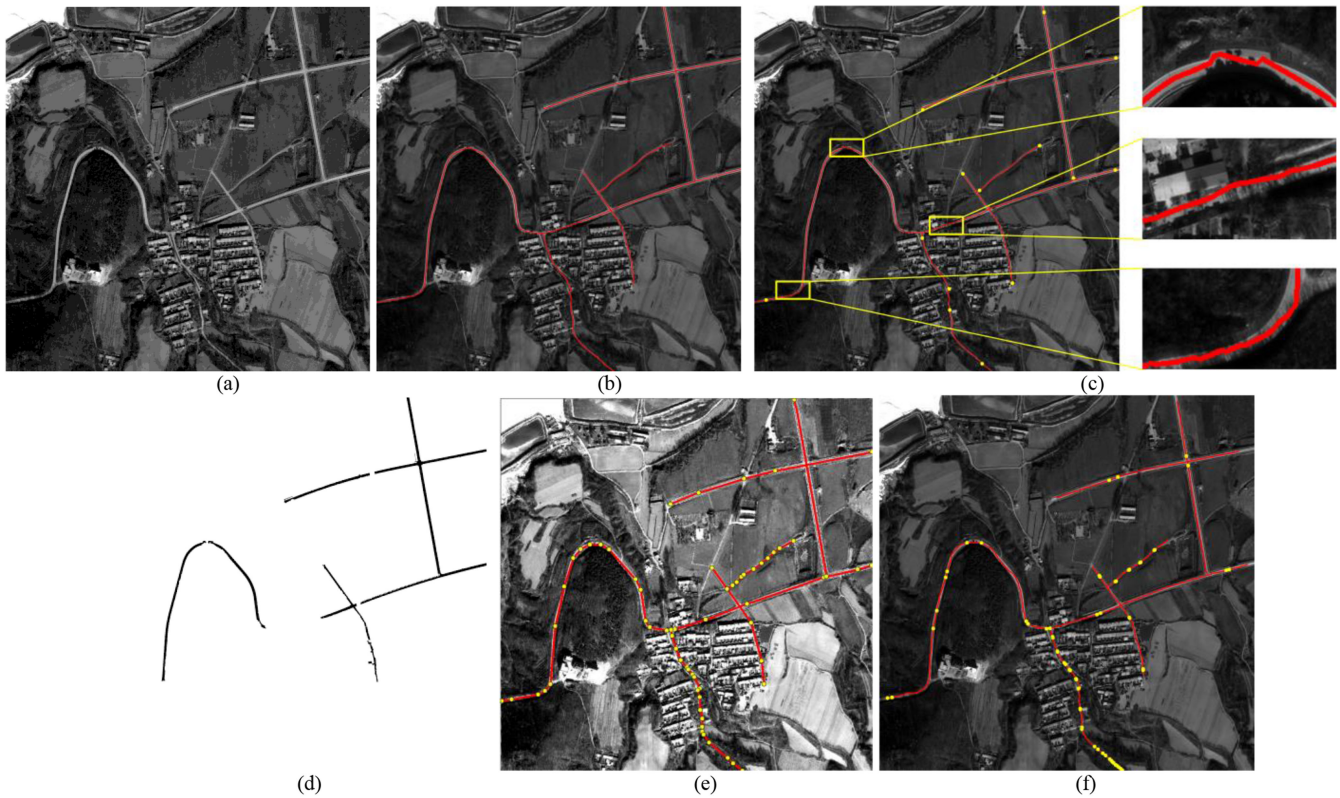
Fig. 12.   Third study area. (a) Input image. (b) Overlaid ground truth data. (c) Results of the proposed method. (d) Results from eCognition. (e) Results from ERDAS. (f) Results of the T-shaped template matching method.

Although the road point is not guaranteed to be at the center of the road, the error is within an acceptable range. However, Fig. 12(e) and (f) need to make supplementary points at the curve to ensure the accuracy of tracking, and the degree of automation is low.

Experiment four: The input data constitute a high-resolution remote sensing images image with a ground spatial resolution of 1.0 m, and the size of the image is 2000×2000 pixels. The first enlarged view in Fig. 13(c) is the intersection area where both the horizontal road and the vertical road center have a completed and clear road centerline. Therefore, the area shown in the figure should be tracked by four roads. The second enlarged view is a roundabout, which mainly reflects two problems.

1) The roundabout is connected to many roads, and so it is difficult to control the tracking direction after entering the roundabout, which is very likely to cause a tracking error. In this article, the MLSOH descriptor is used to determine the approximate road tracking direction, the sector descriptor is used to adjust and verify the tracking points, and contralateral tracking points are used to constrain the current tracking direction dynamically to ensure that tracking is carried out in the predetermined direction; thus, the extraction of the roundabout is realized.

2) The horizontal roads in this area show different characteristics on both sides of the roundabout: the road on the left of the roundabout is a two-way four-lane road with a fence in the middle, which is regarded as two roads. The road to the right of the roundabout is a two-way, two-lane

road with no fence in the middle. We consider it to be one road.

In this article, extraction is based on the right side of the road, and so some roads are missing at the bottom of the roundabout. Some of the road segment texture information in the image is very similar to the background, resulting in many missing regions in the object-oriented road extraction results, and many other features with the same road features are extracted [see Fig. 13(d)]. Fig. 13(e) and (f) require more manual input points to extract roundabouts.

C. Discussion

1) Selection of Experimental Images and Analysis of Applicability of Algorithms: The road tracking method proposed in this article is mainly applicable to high-resolution satellite images with a resolution higher than 1 m and roads of certain widths. To verify the effectiveness of the proposed algorithm, we selected four images with resolutions of 0.5, 0.8 (two images), and 1 m, covering urban, suburban, and country areas, and the road types include straight roads, detours, variational roads, partially or totally shaded roads and roundabouts. Road noise includes full occlusion and semi-occlusion caused by building and tree shadows, vehicles, and viaducts. Thus, the experimental data selected in this article have a certain representativeness.

The proposed method is robust enough in many scenarios. It can be used for semi-automatic road extraction in urban and rural areas, and it is planned to be used in engineering applications to
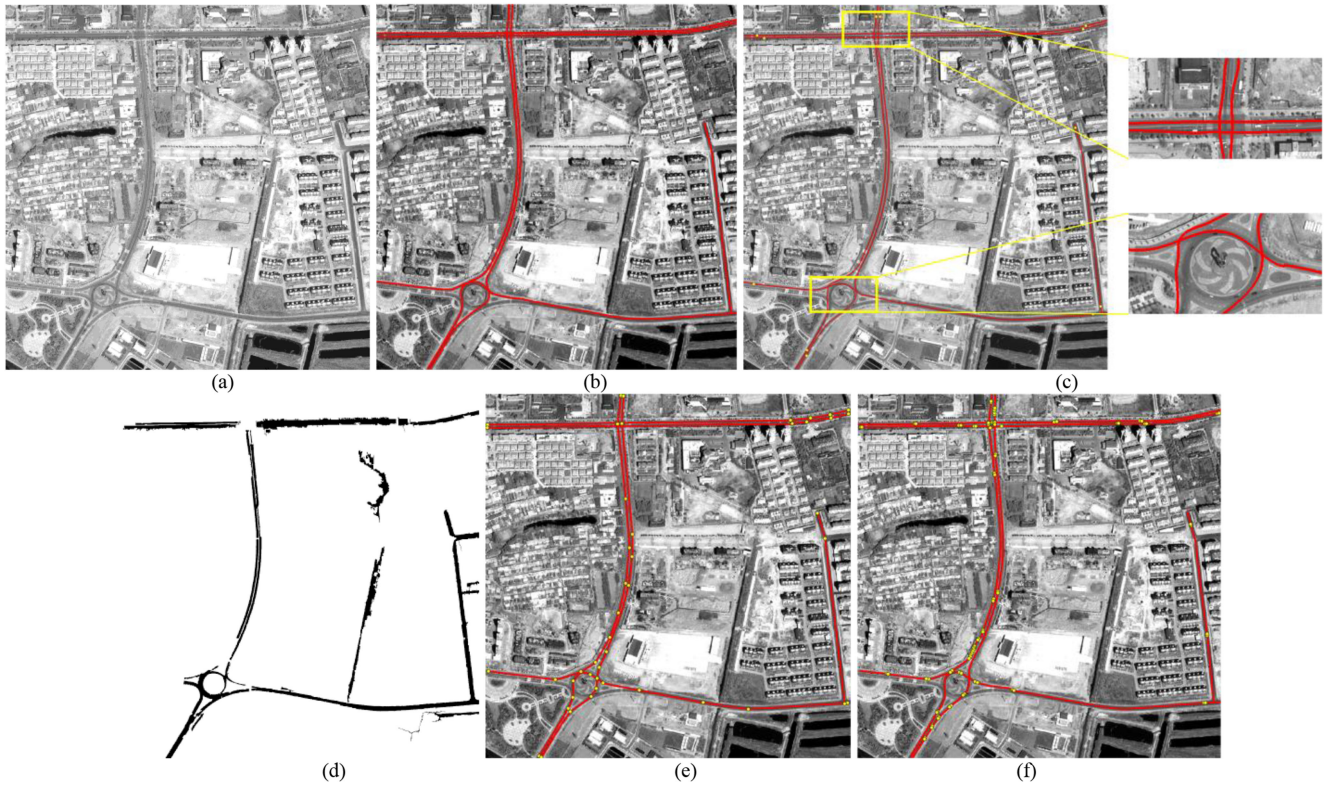
Fig. 13.   Fourth study area. (a) Input image. (b) Overlaid ground truth data. (c) Results of the proposed method. (d) Results from eCognition. (e) Results from ERDAS. (f) Results of the T-shaped template matching method.

reduce the workload of road information extraction practitioners. However, the proposed method also has some limitations. For example, the algorithm in this article has a good extraction effect for the road with a certain width, but for the road with a narrow width, the extraction effect is not very ideal. So that in rural areas, the research object selected in this article is a main road with a wide width; internal roads in villages and mountain roads have not been studied because, in such villages, the shadows of buildings are irregular and, for such roads, the width is usually narrow. The information captured by the sector descriptor is limited, and the anti-noise ability is poor. Moreover, the distribution of trees, buildings, and shadows is irregular, and some road sections are blocked by large areas of trees and their shadows, resulting in the loss of structural information of such sections and the sudden change in texture information, which conflicts with the theoretical basis of the algorithm in this article. Similarly, most of the roads in the forest are blocked by trees. It is extremely difficult to extract the geometric and texture information of the roads from the images. Therefore, the algorithm in this article is currently unsuitable for such roads. The track road has obvious linear information, and so the road extraction process is in line with the idea of this method. However, the orbit is not clear enough in satellite images, and so it may be more suitable to extract orbital roads from aerial images.

2) Selection of Seed Points and Analysis of Supplementary Points: For a manual input point, in general, the seed point input rule must be followed; that is, the structure around the

TABLE IV
EVALUATION TABLE OF THE ROAD EXTRACTION EFFECT OF EXPERIMENT FOUR

Method	Proposed method	ERDAS method	eCognition method	T-shaped method
Completeness (%)	98.93	96.72	84.22	97.54
Correctness (%)	99.61	97.16	87.57	98.38
RMS (pixels)	2.34	3.54	4.63	4.01
Time (s)	54	204	56	57
Number of seeds point	12	45	0	82

road is clear, and there is no obvious vehicle shadow occlusion, which ensures the accuracy of adaptive information acquisition. However, it is necessary to make up points when faults occur in the tracking process. Because of the structure of the fault area is not clear and the occlusion is serious, we select a supplementary point not far in front of the fracture area to ensure the accuracy of the road information. Furthermore, the input points are combined with the original starting point and the end point, and tracking is performed again for road extraction.

3) Accuracy and Automation Analysis: In the local tracking road extraction method, when there are obstacles preventing the extraction of road tracking points, to ensure the accuracy of road extraction, manual participation is often adopted to improve integrity, i.e., the higher the manual participation, the higher the accuracy. In Tables I–IV, the completeness and correctness of road extraction based on template matching (Erdas method and

T-shaped method) are high, and there are no big differences; thus, the key is the degree of human participation. However, in the segmentation and classification process of eCognition, because the data are global images and only a few parameters need to be set, it is often difficult to fully consider the changes of roads in different scenes. Therefore, under occlusion and geometric texture interference, the integrity and quality of road extraction are substantially lower than those of traditional template matching methods. Therefore, the method in this article guarantees the accuracy of road extraction, and the number of manual participants is 1/3 and 1/19 for the Erdas algorithm and the T-shaped template, respectively, which greatly improves the degree of automation of road extraction and fully demonstrates the reliability of our method through experimental verification.

IV. CONCLUSION

In this article, a new type of road tracking method that combines the MLSOH and sector descriptors is proposed. This article employs different types of experimental data to verify the effectiveness of the proposed algorithm. The results demonstrate that for roads with a certain width, the proposed method has universality applicable and can extract a complete road network under the interference of noise, such as parking lots, buildings, trees, and partial shadows over the road. Compared with other methods, it has obvious advantages of high automation and high accuracy. However, many problems in this article need to be improved. For example, the MLSOH descriptor used in this article can provide direction constraints for roads under partial shadows. For large shadows that are uniformly grey without any reference features, the effect of the descriptor is not satisfactory, and information often needs to be supplemented. Moreover, the problem of road extraction has not been solved when there are many vehicle disturbances and instances of building and road texture convergence; thus, problem will be addressed during further algorithm improvement.

REFERENCES

[1] J. B. Mena, "State of the art on automatic road extraction for GIS update: A novel classification," *Pattern Recognit. Lett.*, vol. 24, no. 16, pp. 3037–3058, 2003.

[2] R. Bonnefon, P. Dhrt, and J. Desachy, "Geographic information system updating using remote sensing images," *Pattern Recognit. Lett.*, vol. 23, no. 9, pp. 1073–1083, 2002.

[3] W. Shi, C. Zhu, and Y. Wang, "Road feature extraction from remotely sensed image: Review and prospects," *Acta Geodatica et Cartographica Sin.*, vol. 30, no. 3, pp. 257–262, 2001.

[4] Q. Li, L. Chen, M. Li, S. L. Shaw, and A. Nuchter, "A sensor-fusion drivable-region and lane-detection system for autonomous vehicle navigation in challenging road scenarios," *IEEE Trans. Veh. Technol.*, vol. 63, no. 2, pp. 540–555, Feb. 2014.

[5] M. Mokhtarzade and M. J. V. Zoej, "Road detection from high-resolution satellite images using artificial neural networks," *Int. J. Appl. Earth Observation Geoinf.*, vol. 9, no. 1, pp. 32–40, 2007.

[6] R. Alshehhi and P. R. Marpu, "Hierarchical graph-based segmentation for extracting road networks from high-resolution satellite images," *ISPRS J. Photogrammetry Remote Sens.*, vol. 126, pp. 245–260, 2017.

[7] S. Callier and H. Saito, "Automatic road area extraction from printed maps based on linear feature detection," *IEICE Trans. Inf. Syst.*, vol. 95, pp. 1758–1765, 2012.

[8] F. Ameri and M. J. V. Zoej, "Road vectorisation from high-resolution imagery based on dynamic clustering using particle swarm optimization," *Photogrammetric Rec.*, vol. 30, no. 152, pp. 363–386, 2015.

[9] M. D. Mura, L. Pralon, G. Vasile, M. D. Mura, J. Chanussot, and N. Sesaic, "Simultaneous extraction of roads and buildings in remote sensing imagery with convolutional neural networks," *ISPRS J. Photogrammetry*, vol. 130, pp. 139–149, 2017.

[10] Z. L. Miao, W. Z. Shi, and H. Zhang, "A road centerline extraction algorithm from high resolution satellite imagery," *J. China Univ. Mining Technol.*, vol. 42, no. 5, pp. 887–892, 2013.

[11] C. Akinlar and C. Topal, "Edlines: A real-time line segment detector with a false detection control," *Pattern Recognit. Lett.*, vol. 32, no. 13, pp. 1633–1642, 2011.

[12] M. Maboudi, J. Amini, M. Hahn, and M. Saati, "Road network extraction from VHR satellite images using context aware object feature integration and tensor voting," *Remote Sens.*, vol. 8, no. 6, 2016, Art. no. 637.

[13] T. Blaschke, "Quantifying the robustness of fuzzy rule sets in object-based image analysis," *Int. J. Remote Sens.*, vol. 32, no. 22, pp. 7359–7381, 2011.

[14] W. Shi, Z. Miao, and J. Debayle, "An integrated method for urban main-road centerline extraction from optical remotely sensed imagery," *IEEE Trans. Geosci. Remote Sens.*, vol. 52, no. 6, pp. 3359–3372, Jun. 2014.

[15] Z. Miao, W. Shi, H. Zhang, and X. Wang, "Road centerline extraction from high-resolution imagery based on shape features and multivariate adaptive regression splines," *IEEE Geosci. Remote Sens. Lett.*, vol. 10, no. 3, pp. 583–587, May 2013.

[16] X. Huanga and L. Zhanga, "Road centreline extraction from high resolution imagery based on multiscale structural features and support vector machines," *Int. J. Remote Sens.*, vol. 30, no. 8, pp. 1977–1987, 2009.

[17] J. D. Wegner, J. A. Montoya-Zegarra, and K. Schindler, "A higher-order CRF model for road network extraction," in *Proc. IEEE Conf. Comput. Vision Pattern Recognit.*, 2013, pp. 1698–1705.

[18] D. Yin, S. Du, S. Wang, and Z. Guo, "A direction-guided ant colony optimization method for extraction of urban road information from very-high-resolution images," *IEEE J. Sel. Top. Appl. Earth Observ. Remote Sens.*, vol. 8, no. 10, pp. 4785–4794, Oct. 2015.

[19] M. Maboudi, J. Amini, M. Hahn, and M. Saati, "Object-based road extraction from satellite images using ant colony optimization," *Int. J. Remote. Sens.*, vol. 38, no. 1, pp. 179–198, 2017.

[20] M. Maboudi, J. Amini, S. Malihi, and M. Hahn, "Integrating fuzzy object based image analysis and ant colony optimization for road extraction from remotely sensed images," *ISPRS J. Photogrammetry Remote Sens.*, vol. 138, pp. 151–163, 2018.

[21] B. Liu, H. Wu, Y. Wang, and W. Liu, "Main road extraction from ZY-3 grayscale imagery based on directional mathematical morphology and vgi prior knowledge in urban areas," *PLoS One*, vol. 10, no. 9, 2015, Art. no. e0138071.

[22] D. Chaudhuri, N. K. Kushwaha, and A. Samal, "Semi-automated road detection from high resolution satellite images by directional morphological enhancement and segmentation techniques," *IEEE J. Sel. Topics Appl. Earth Observ. Remote Sens.*, vol. 5, no. 5, pp. 1538–1544, Oct. 2012.

[23] X. Hu, Y. Li, J. Shan, J. Zhang, and Y. Zhang, "Road centerline extraction in complex urban scenes from Lidar data based on multiple features," *IEEE Trans. Geosci. Remote Sens.*, vol. 52, no. 11, pp. 7448–7456, Nov. 2014.

[24] X. Y. Hu, Z. X. Zhang, and J. Q. Zhang, "An approach of semi-automated road extraction from aerial images based on template matching and neural network," *Int. Archives Photogrammetry Remote Sens.*, vol. 33, pp. 994–999, 2000.

[25] S. Leninisha and K. Vani, "Water flow based geometric active deformable model for road network," *ISPRS J. Photogrammetry Remote Sens.*, vol. 102, pp. 140–147, 2015.

[26] J. X. Zhang, X. G. Lin, Z. J. Liu, and J. Shen, "Semi-automatic road tracking by template matching and distance transformation in urban areas," *Int. J. Remote Sens.*, vol. 32, no. 23, pp. 8331–8347, 2011.

[27] X. Lin and Z. Liu, "Semi-automatic extraction of ribbon roads from high resolution remotely sensed imagery by T-shaped template matching," *Geomatics Inf. Sci. Wuhan Univ.*, vol. 7147, no. 3, pp. 293–296, 2009.

[28] G. Fu, H. R. Zhao, C. Li, and L. M. Shi, "Road detection from optical remote sensing imagery using circular projection matching and tracking strategy," *J. Indian Soc. Remote Sens.*, vol. 41, no. 4, pp. 819–831, 2013.

[29] C. Xu and J. L. Prince, "Gradient vector flow: A new external force for snakes," in *Proc. IEEE Comput. Soc. Conf. Comput. Vis. Pattern Recognit.*, 1997, pp. 66–71.

[30] Y. Nakaguro, S. S. Makhanov, and M. N. Dailey, "Numerical experiments with cooperating multiple quadratic snakes for road extraction," *Int. J. Geographical Inf. Sci.*, vol. 25, no. 5, pp. 765–783, 2011.

[31] S. Osher and J. A. Sethian, "Fronts propagating with curvature-dependent speed: Algorithms based on Hamilton-Jacobi formulations," *J. Comput. Phys.*, vol. 79, no. 1, pp. 12–49, 1988.

[32] M. Rajeswari, K. S. Gurumurthy, S. Omkar, J. Senthilnath, and L. P. Reddy, "Automatic road extraction using high resolution satellite images based on level set and mean shift methods," in *Proc. IEEE 4th Int. Conf. Comput.*, 2014, pp. 1–7.
[33] J. Dai, Z. Li, L. I. Jinwei, and X. Fang, "A line extraction method for chain code tracking with phase verification," *Acta Geodaetica Geophys.*, vol. 46, pp. 218–227, 2017.
[34] L. Xu, C. Lu, Y. Xu, and J. Jia, "Image smoothing via l0 gradient minimization," *ACM Trans. Graph.*, vol. 30, no. 6, pp. 1–12, 2011.
[35] R. L. Tan, Y. C. Wan, F. Yuan, and G. Li, "Semi-automatic road extraction of high resolution remote sensing images based on circular template," *Bull. Surv. Map.*, vol. 10, pp. 63–66, 2014.
[36] G. Li, J. An, and C. Chen, "Automatic road extraction from high-resolution remote sensing image based on bat model and mutual information matching," *J. Comput.*, vol. 6, no. 11, pp. 2417–2426, 2011.
[37] Z. L. Miao, B. Wang, W. Z. Shi, and H. Zhang, "A semi-automatic method for road centerline extraction from VHR images," *IEEE Geosci. Remote Sens. Lett.*, vol. 11, no. 11, pp. 1856–1860, Nov. 2014.
[38] Y. Yun and C. Q. Zhu, "Extracting road centerlines from high resolution satellite images using active window line segment matching and improved SSDA," *Int. J. Remote Sens.*, vol. 31, no. 9, pp. 2457–2469, 2010.
[39] C. Wiedemann, C. Heipke, H. Mayer, and O. Jamet, "Empirical evaluation of automatically extracted road axes," in *Proc. Empirical Eval. Techn. Comput. Vis.*, 1998, pp. 172–187.
[40] C. Wiedemann and H. Ebner, "Automatic completion and evaluation of road networks," *Int. Arch. Photogrammetry Remote Sens.*, vol. 33, pp. 979–986, 2000.

Tingting Zhu received the B.Eng. degree in remote sensing science and technology from Liaoning Technical University, Fuxin, China, in 2017. She is currently working toward the M.Sc. degree with the School of Surveying and Geosciences, Liaoning Technical University.

Her research interest includes remote sensing image information processing.

Yang Wang received the B.Eng. degree in remote sensing science and technology from Liaoning Technical University, Fuxin, China, in 2017. She is currently working toward the M.Sc. degree with the School of Surveying and Geosciences, Liaoning Technical University.

Her research interest includes remote sensing image information processing.

Rongchen Ma received the B.Eng. degree in remote sensing science and technology from Liaoning Technical University, Fuxin, China, in 2018. She is currently working toward the M.Sc. degree in the School of Surveying and Geosciences, Liaoning Technical University.

Her research interest includes remote sensing image information processing.

Jiguang Dai received the B.Eng. degree in land resource management from China Agricultural University, Beijing, China, in 2001, the M.Sc. degree from Lanzhou University, Lanzhou, China, in 2006, and the Ph.D. degree from Liaoning Technical University, Fuxin, China, in 2013.

From 2006 to 2014, he was a Lecturer with the School of Surveying and Geosciences, Liaoning Technical University. He is currently an Associate Professor with the School of Surveying and Geosciences, Liaoning Technical University. His research interest includes remote sensing image information processing.

Xinxin Fang received the M.Sc. degree in surveying and mapping engineering from Liaoning University of Engineering and Technology, Fuxin, China, 2017.

His research interest includes remote sensing image information processing.